RP Current Trends In Applied Sciences (e-ISSN: 2583-7486)
Vol. 5, No. 2 (April – June 2026) pp. 89–94

RESEARCH PLATEAU PUBLISHERS

Cite this article: K. Lohar, P. Mishra, S.K. Sahu, Comparative microstructure, texture, and property anisotropy of As deposited and heat-treated DMLS Inconel 718, *RP Cur. Tr. Appl. Sci*. **5** (2026) 89–94.

Original Research Article

Comparative microstructure, texture, and property anisotropy of As deposited and heat-treated DMLS Inconel 718

Kalyani Lohar*, Punyapriya Mishra, Santosh Kumar Sahu

Veer Surrendra Sai University of Technology, Burla, Sambalpur, Odisha, India
*Corresponding author, E-mail: kalyaniloharphd21@vssut.ac.in

ARTICLE HISTORY
Received: 16 April 2026
Revised: 27 May 2026
Accepted: 27 May 2026
Published: 13 June 2026

KEYWORDS
Additive manufacturing;
Laser powder bed fusion;
Heat treatment;
Microstructure;
X-ray diffraction;
Inconel 718.

ABSTRACT
Direct Metal Laser Sintered (DMLS) Inconel 718 microstructural evolution was studied to gain an insight into the behavior of the material in their as deposited and heat treated (HT) states. In this research, an exhaustive range of characterization techniques, including X-ray diffraction (XRD), optical microscopy (OM), and scanning electron microscopy (SEM), were used to examine the grain structure, texture, and phase composition. These tests show that parts produced via DMLS have similar density and porosity levels as traditional cold-rolled material, thus proving itself as not an unstable process. The results of surface roughness and microhardness were further shown to have accumulated orientation effect on mechanical inhomogeneity. The significance of post process heat treatment in this work is the refinement of microstructure, re-orientation of grains and coalescence of grains, which enhances the basic knowledge of processing structure property relationships in additively manufactured super-alloys.

1. Introduction

The need to have highly efficient engineering materials in aerospace engineering has necessitated the critical research and development of the super alloy systems that can enhance the mechanical stability in highly demanding functional conditions. Of these, nickel-based super-alloy capture a very important place, due to their very remarkable combination of microstructural stability to higher temperature strength. Specifically, Inconel 718 (IN718) has emerged as one of the most popular in turbine engines and compressor systems, as a significant percentage of the overall alloy weight in contemporary jet propulsion platforms [1,2]. Nickel-based super-alloys, especially IN718 are widely used in aerospace parts like turbine blades and compressor casings due to the fact that they maintain high strength, high creep strength, and strong oxidation and corrosion resistance at temperatures of up to 650 C. These elements are normally of complex geometry and they are subjected to harsh mechanical and thermal loads in operation. Nevertheless, conventional manufacturing paths tend to have restrictions in creating such subtle forms in the same breath as they deliver the desired performance levels. Consequently, transition towards high-technology manufacturing methods to suit more complex design and challenging operational conditions has increased [3].

Laser Powder Bed Fusion (LPBF) consolidates successive layers of pre-alloyed metallic powder through selective melting by a focused laser beam as a source guided by a digitally defined scan pattern derived from a three-dimensional computer-aided design model. Each layer, typically between 20 to 80 μm in thickness with relevant to the machine specification, which is fused to the preceding layer by the formation and rapid solidification of a melt pool, the dimensions and thermal process of which are governed by laser power, scan speed, hatch spacing, and layer thickness. The energy density delivered to the powder bed indicates the degree of sintering, melt pool stability, and the reduction of negatively metallurgical bond between adjacent tracks and successive layers as shown in Figure 1 [4, 5].

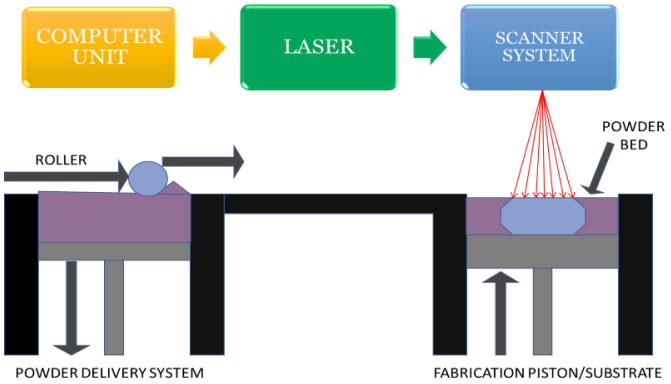

Figure 1: Schematic diagram of DMLS fabrication process.

The process requires extremely higher cooling rates, typically in the range of 10^5 - 10^7 K/s, which arises from the rapid thermal gradients between the melt pool and the adjacent area of the fused material [6]. These conditions remarkably influence the as built sample microstructure generated by LPBF, acquire a cellular or columnar grain structure with a feature build-direction texture emerging from epitaxial grain growth alongside the thermal gradient. The resulting microstructure differs substantially from that obtained by

traditional casting or forging method, and this distinction has motivated investigation into how process parameters and post-build heat treatments can be optimised to improve the final mechanical properties [7].

2. Materials and method

Post heat treatment process, which involves a combination of homogenisation (HSA), solution annealing (SA), and double ageing (DA) in compliance with the AMS 5664 standard. Initially, a cuboid specimen of 6mm × 6mm × 5 mm was fabricated through the DMLS technique using the IN718 powder [8]. The XRD spectra of IN718 powder are depicted in Figure 5, where only the {111}, {200}, and {220} distinct peaks are visible, which means the powder quality with no adulteration. After various experimentation, an optimised process parameter set was selected i.e. laser power (LP) at 350 W, 1500 mm/s scanning speed (SS), 120 µm hatch spacing (HS), and a layer thickness (LT) of 0.04 mm. The experiments were conducted under an argon atmosphere. [9]. The AB samples were subjected to heat treatments as per AMS 5664 standard to reduce the internal stresses whilst removing the microstructural defects and laves phases to impart isotropic behaviour in the manufactured part. With the help of muffle furnace, the samples were initially heated up to 1080°C with a holding time for 1 hour, thereafter cooled to 960°C with a holding time for 1 hour. then air cooled to room temperature to 30°C. Again, the samples were subjected to double aging at 720°C for 8 hours and then at 620°C for 8 hours, followed by cooling to room temperature [10]. After the heat treatments, the AB and HT specimen's density were measured via Archimedes' principle. The microhardness values were determined from Vickers testing (load 200gf and dwell time 15 sec). Moreover, the variation of the microstructural elements under various conditions (AB, and HT) were evaluated through FESEM.

3. Results and discussion

3.1 Porosity measurement

The mass and experimental density of As-built (AB) sample were 1.98 g and 7.82 g/cm³, while Heat-treated (HT) sample with 2.066 g and 7.9 g/cm³ measured values. The estimated porosity was approximately 4.42% for AB sample and 3.44% for HT sample, indicating reduction in porosity and improving the microstructural uniformity after heat treatment. The whole mass rise in HT sample did not affect the reduction in porosity although it shows better densification after thermal processing. The density estimated through Archimedes' principle can face inaccuracy due to up-thrust problems as well as air entrapping and liquid penetration into pores. Gas assisted atomization presents powder particles with spherical morphology and less internal void and satellite features.

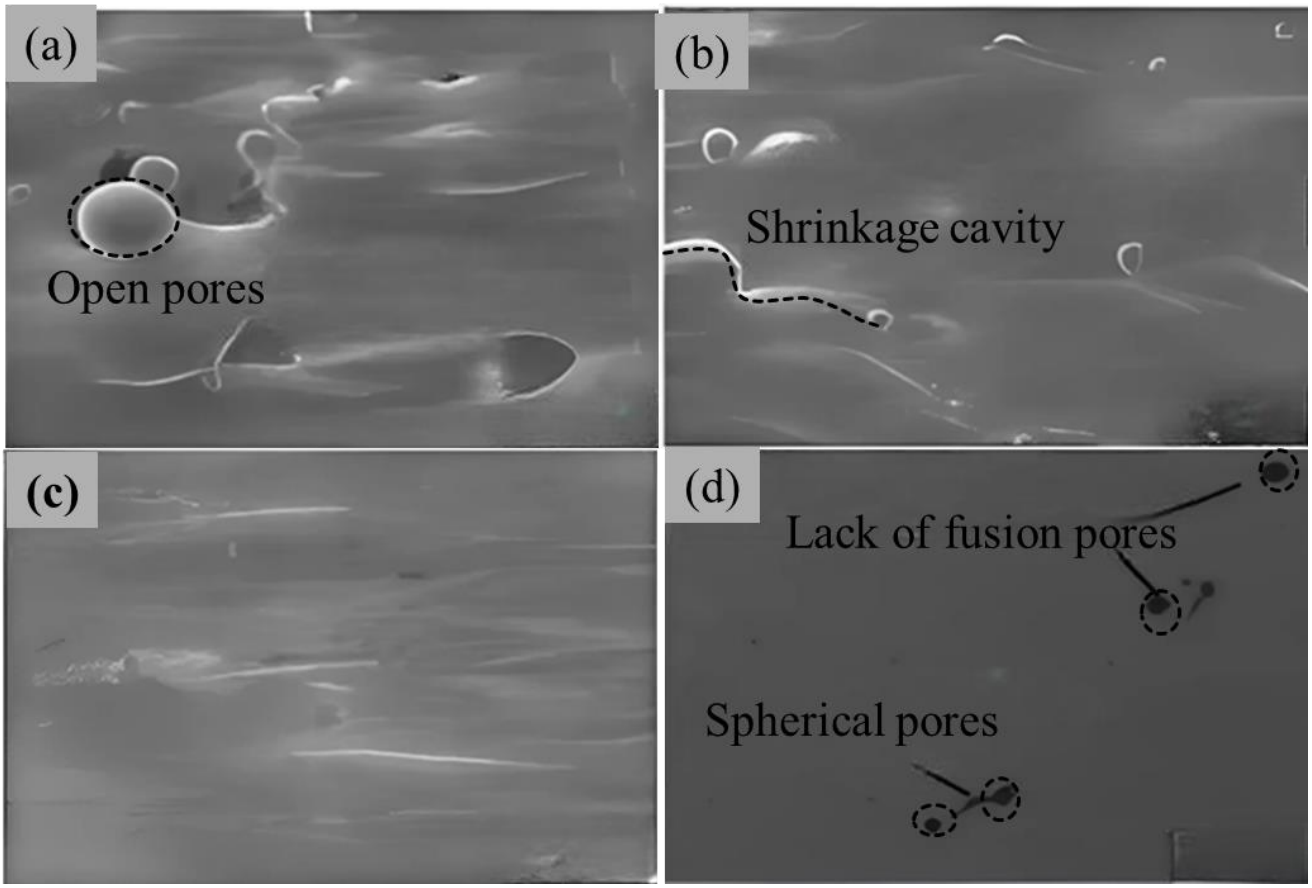

Figure 2: SEM morphology of different defects.

Porosity emerging from lack-of-fusion which is between adjacent melt tracks or from keyhole instability at higher energy densities, indicates a primary defect type in LPBF IN718 as shown in Figure 2. Lack-of-fusion pores, which tends to be irregular and elongated and particularly adverse to mechanical performance due to their tendency to perform as fatigue crack initiation sites [14]. Optimized process parameters that balances full sintering with melt pool stability hence necessary for making compact components with governed defect populations.

3.2 Microstructure analysis and elemental analysis

Figure 3(a, b) demonstrate the state of the AB sample, where the microstructure primarily consists of a γ matrix scattered with laves phase. The AB sample also revealed detectable sub-grain boundary networks along with enhanced columnar and equiaxed dendritic structure.

After subjecting the material to heat treatment, the grain boundary regions turned considerably more distinct, attributable to the nucleation and growth of coarse plate-like precipitates, prominently a cracked δ-phase morphology, as shown in Figure 3(c, d). A positive correlation was identified between the existence of the Laves phase and the beginning of brittleness in IN718. These intermetallic precipitates enriched with Nb, Mo, and Ti elements preferably during solidification or extreme temperature, gradually depleting niobium from the nearby matrix. This depletion critically quashes γ″ precipitation, which serves as the primary strengthening mechanism in this alloy.

Formed in the interdendritic areas and grain boundaries, Laves phase elements act as the centres of stress and favourable places of crack formation. These critical brittle particles, under mechanical load, promote microcrack growth along with the grain boundaries, thus reducing ductility, fracture toughness, and fatigue strength [15]. To this end, the formation of laves phases continues to be a key contributor to brittleness and the deterioration of mechanical behavior in such alloys. The Laves phase in the AB state depicted in Figure 3 (a, b) was followed by solution aging (SA) treatment wherein the phase had elongated morphology which disintegrated and dissolved partially subsequently changing into coarser separate particles. Further doubling of the aging resulted in the almost complete removal of the Laves phase, giving a much more homogeneous and uniform microstructural distribution.

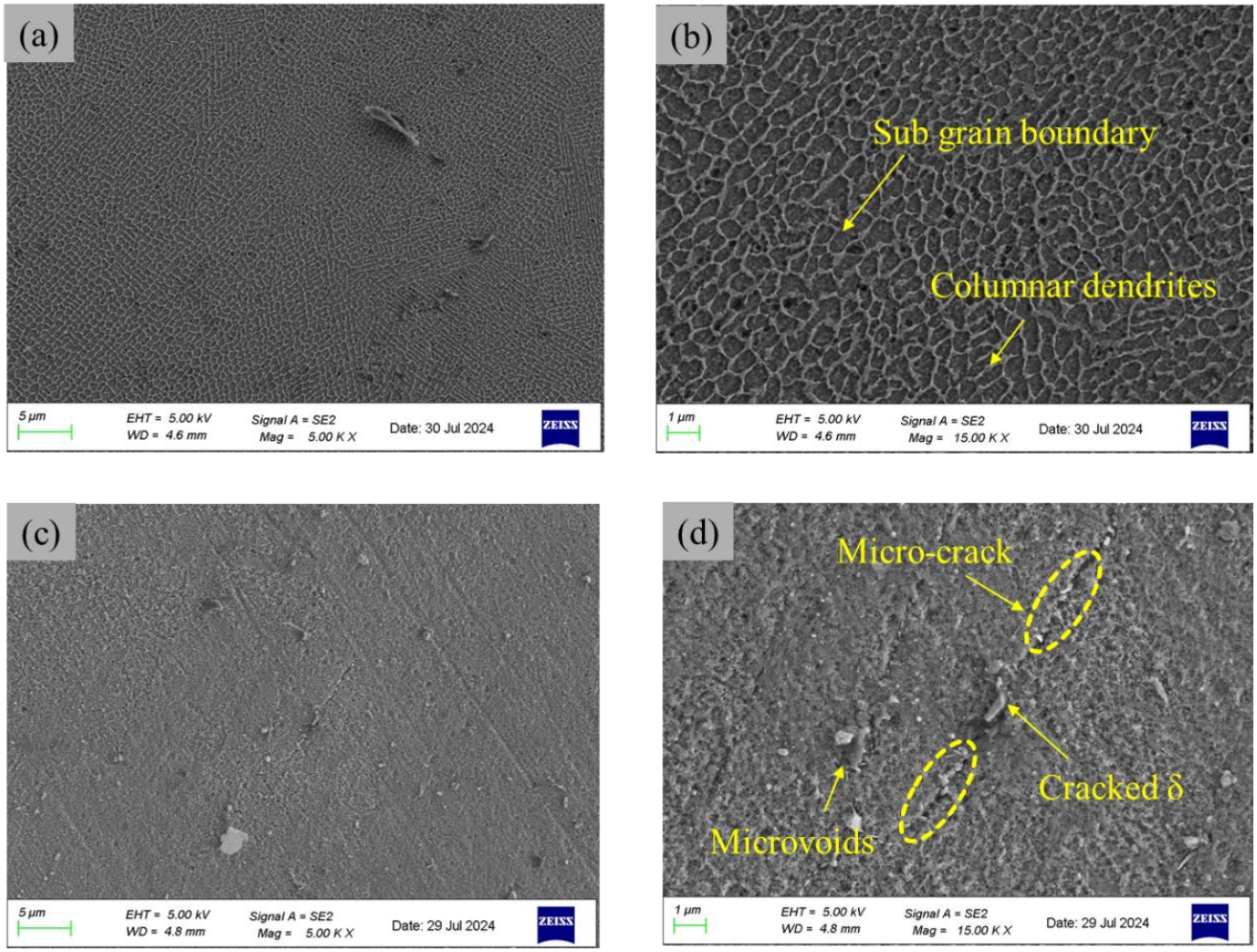

Figure 3: SEM image of AB sample (a, b) and HT sample (c, d).

3.3 EDS analysis

The processes of the precipitated phases were examined by use of Energy Dispersive Spectroscopy (EDS) and the elemental segregation of the different processing conditions such as the AB and HT specimens were determined with varying processing conditions. Figure 4(a) shows the EDS spectrum and maps of elemental distributions of IN718 produced by DMLS process. Among the observed elements, Ni and Cr is highly important in ensuring stability of high temperature and corrosion resistance, with Nb, Ti, and Mo being the main elements that enhance strength of the alloy by precipitation hardening mechanism and enhancing its creep resistance. A comparative EDS analysis of the heat-treated DMLS specimen is shown in Figure 4(b). The elements value is quantitative and indicates that the Ni content is growing to 46.4 wt. %, Nb is growing to 6.2 wt. % and Ti is growing to 1.4 wt. %. Having used heat treatment, the distribution of alloying elements throughout the microstructure becomes more

homogeneous, indicating that effective phase stabilization and solid-state diffusion had occurred. This disorder is believed to be the most metal-favourable towards the formation of strengthening precipitate phases. The simultaneous existence of high Ni, Nb, and Mo levels, and even distribution of the elements, altogether contribute to increased phase stability, better mechanical behavior, and increased thermal degradation resistance. The stable retention of Mo at 2.7 wt. % and Al at 0.7 wt. % further supports the ability of the alloy to resist high-temperature creep and oxidative conditions [16].

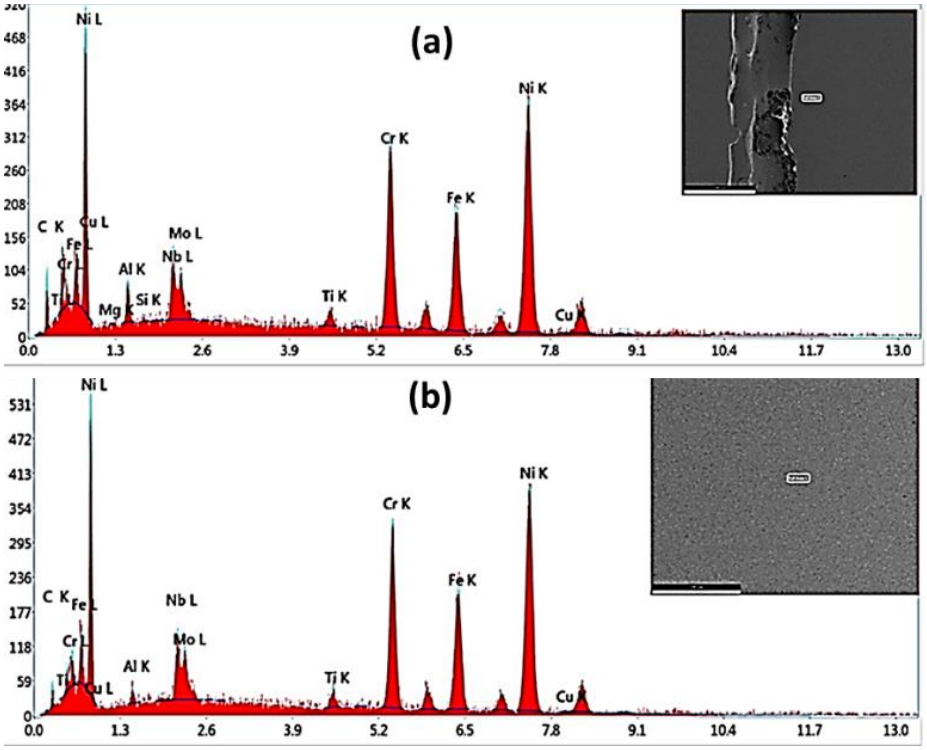

Material(→) Element(↓)	DMLS Inconel 718	Heat treated DMLS Inconel 718
Ni	42.7	46.4
Cr	14.9	16.9
Fe	14.0	15.7
Al	1.6	0.7
Ti	1.0	1.4
Nb	5.4	6.2
Mo	2.1	2.7
C	16.9	8.9
Cu	1.0	0.7

Figure 4: EDS analysis of (a) AB sample, (b) HT sample.

The sophisticated microstructural features met by heat treatment make this alloy variant a serious competitor in the high-performance demanding applications, such as turbine blades, and aerospace structural parts, where ability to resist high temperatures, fatigue loading and long-lasting material degradation are paramount design concerns.

3.4 XRD analysis

The crystallographic study of the AB and HT specimens shows the existence of prominent diffraction planes, namely, the planes: {111} and the planes: {200} and the plane: {220} as presented in Figure 5. The same planes were also found in the untreated IN718 powder. The sample produced through the DMLS method clarifies the broadening of the peaks after which there was a marginal deviation in the 2 -values, all of which suggest a reduction of grain size.

With a continuously increasing temperature, the diffraction peaks are becoming clearer and narrower, which means that the internal structure of the crystal is becoming relaxed. Having a uniform distribution of phases is promoted by heat treatment, which also leads to lattice stability and a quantifiable reduction in residual stresses in the material [17].

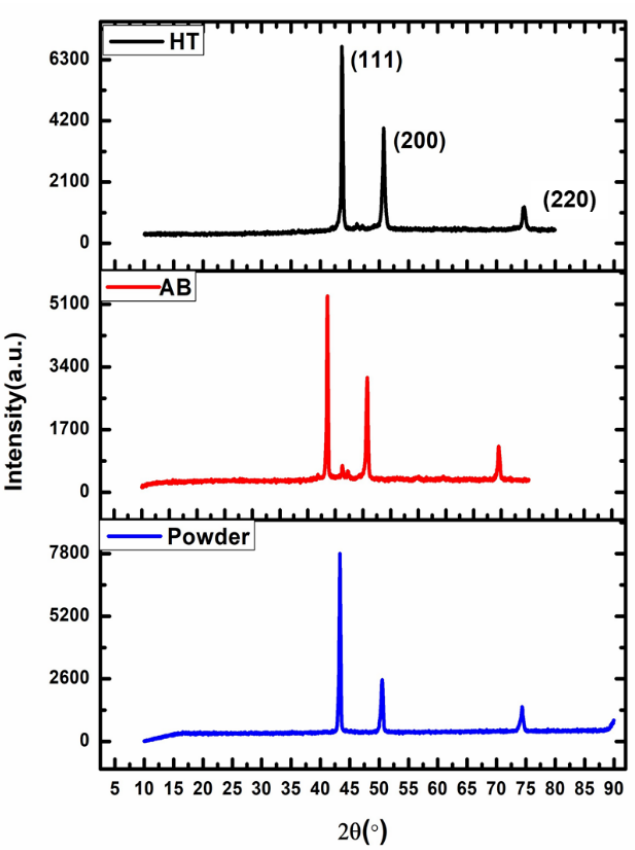

Figure 5: XRD pattern.

3.5 Microhardness

Microhardness evaluation plays an important role in determining localized mechanical property, especially in components produced via additive manufacturing. The material reaches a high degree of hardness (above 500 HV) in the heat-treated (HT) condition and then stabilizes at a plateau level (around 400 HV). The collaborative interface between precipitation hardening and microstructural stability and homogenisation of the matrix, together with the contribution of the excellent mechanical integrity of aerospace turbine engineered components, is realised in such remarkable improvement [18, 19].

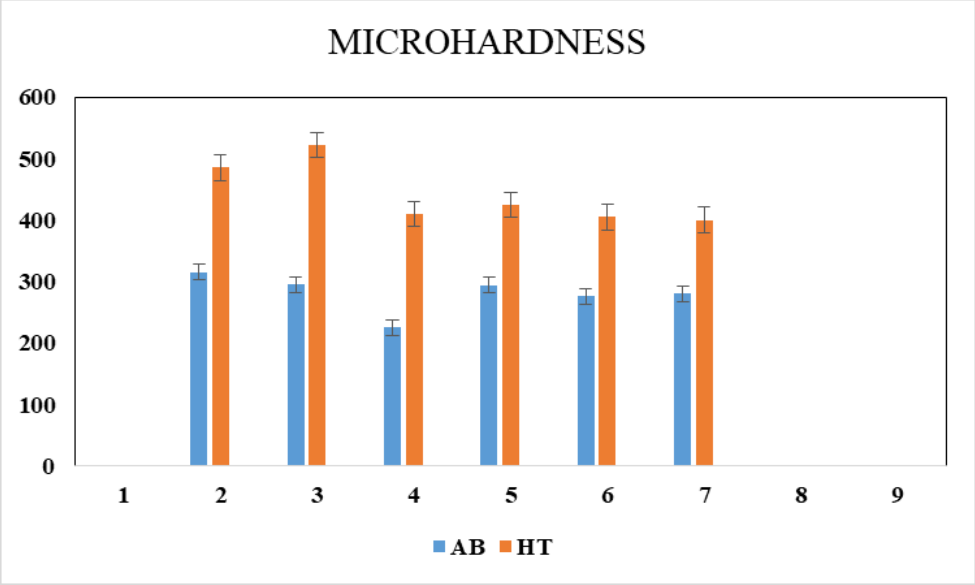

Figure 6: Microhardness value.

Figure 6 indicates that the AB specimen has a medium hardness data of about 300 HV with the columnar dendritic solidification patterns in microstructure, residual thermal stresses applied during the fabrication process and Laves phases precipitation affecting the hardness data. All these contribute to the increase in the microstructural non-uniformities and unevenly distributed grain sizes across the material. Conversely, the heat-treated DMLS IN718 exhibit superior and uniform hardness characteristics, and thus the best prototype to use in the application where high mechanical integrity and high resistance to plastic deformation are required during service [20].

4. Conclusions

- The post-heat treatment of DMLS-fabricated IN718 specimen can remarkably reduce the number of defects of porosity as well as anisotropic behaviour, leading to a much more homogeneous microstructure than its AB counterpart.
- Precipitates were identified and described with the help of FESEM with EDS and XRD analysis which confirmed once again that the γ-phase was predominant.
- The microstructural study revealed a columnar dendritic structure confined within the limits of melt pools, which is the direct result of the directional solidification nature of the DMLS method.
- An anisotropy of the specimen decreased by the heat treatment because the redistribution of the phases became even more homogeneous at the microscopic level.
- The values of the microhardness showed that the post processing heat treatment of the sample produced the highest values (around 311 HV), compared to the as-built sample (around 278 HV), which is a confirmation of the wisdom of post processing heat treatment in enhancing the mechanical strength of the sample.

Authors' contributions

The author read and approved the final manuscript.

Conflicts of interest

The author declares no conflict of interest.

Funding

This research received no external funding.

Data availability

No new data were created.

References

[1] F. Marin, A.F. de Souza, A. Mikowski, L.H.G. Fontanella, P. Soares, L.N.L. de Lacalle, Energy density effect on the interface zone in parts manufactured by laser powder bed fusion on machined bases, *Int. J. Precis. Eng. Manuf.-Green Technol*. **10** (2023) 905–923.

[2] S. Kim, H. Choi, J. Lee, S. Kim, Room and elevated temperature fatigue crack propagation behavior of Inconel 718 alloy fabricated by laser powder bed fusion, *Int. J. Fatigue* **140** (2020) 105802.

[3] J. Zhang, M. Bermingham, J. Otte, Y. Liu, M. Dargusch, Towards uniform and enhanced tensile ductility of additively manufactured Ti−5Al−5Mo−5V−3Cr alloy through designing gradient interlayer deposition time, *Scr. Mater*. **223** (2023) 115066.

[4] H. Yang, L. Meng, S. Luo, Z. Wang, Microstructural evolution and mechanical performances of selective laser melting Inconel 718 from low to high laser power, *J. Alloys Compd*. **828** (2020) 154473.

[5] P.E. May, M. White, A. Bordin, L. Ednie, R. Huff, S. Vunnam, R.J. Lancaster, Influence of heat treatment on the high

temperature properties of Inconel 718 fabricated via laser beam powder bed fusion, *J. Mater. Res. Technol*. **36** (2025) 9881–9897.
[6] J. Yang, H. Yu, H. Yang, F. Li, Z. Wang, X. Zeng, Prediction of microstructure in selective laser melted Ti_6Al_4V alloy by cellular automaton, *J. Alloys Compd*. **748** (2018) 281–290.
[7] F. Soffel, D. Eisenbarth, E. Hosseini, K. Wegener, Interface strength and mechanical properties of Inconel 718 processed sequentially by casting, milling, and direct metal deposition, *J. Mater. Process. Technol*. **291** (2021) 117021.
[8] L.A. Chicos, C. Lancea, S.M. Zaharia, G. Cempura, A. Kruk, M.A. Pop, Effects of homogenization heat treatment on microstructure of Inconel 718 lattice structures manufactured by selective laser melting, *Materials* **18** (2025) 4149.
[9] D. Panov, G. Permyakov, S. Naumov, V. Mirontsov, E. Kudryavtsev, L. Sun, G. Salishchev, The effect of post-deposition heat treatment on the microstructure, texture, and mechanical properties of Inconel 718 produced by hybrid wire-arc additive manufacturing with inter-pass forging, *Metals* **15** (2025) 78.
[10] S. Naskar, S. Suryakumar, B.B. Panigrahi, Post-processing of Inconel 718 superalloy by laser-based powder bed fusion: Microstructures and properties evaluation, *Mater. Sci. Eng. A* **921** (2025) 147601.
[11] S. Zhang, Y. Wang, L. Lv, H. Deng, J. Lin, B. Lv, F. Liu, Effect of heat treatment on the microstructure and mechanical anisotropy of selective laser-melted Inconel 718 alloy, *Mater. Today Commun.* (2025) 113453.
[12] E.M. Fayed, D. Shahriari, M. Saadati, V. Brailovski, M. Jahazi, M. Medraj, Influence of homogenization and solution treatments time on the microstructure and hardness of Inconel 718 fabricated by laser powder bed fusion process, *Materials* **13** (2020) 2574.
[13] B. Farhang, B.B. Ravichander, J. Ma, A. Amerinatanzi, N.S. Moghaddam, The evolution of microstructure and composition homogeneity induced by borders in laser powder bed fused Inconel 718 parts, *J. Alloys Compd.* **898** (2022) 162787.
[14] Q. Jia, D. Gu, Selective laser melting additive manufacturing of Inconel 718 superalloy parts: Densification, microstructure and properties, *J. Alloys Compd*. **585** (2014) 713–721.
[15] M. Rizwan, R. Ullah, J. Lu, J. Wang, Y. Zhang, Z. Zhang, Insight into elongation and strength enhancement of heat-treated LPBF Ni-based superalloy 718 using in-situ SEM-EBSD, *Mater. Sci. Eng. A* **914** (2024) 147163.
[16] P. Kumnaknoppakun, V. Uthaisangsuk, Effect of printing parameters and heat treatments on microstructure development of LPBF manufactured Inconel 718 alloy, *Mater. Perform. Charact.* **13** (2024) 246–262.
[17] L. Ramineni, A. Almotari, M. Ali, A. Algamal, A. Qattawi, Residual stress mapping in heat-assisted additive manufacturing of IN 718: an X-ray diffraction study, *J. Mater. Eng. Perform.* **33** (2024) 4124–4135.
[18] J. Čapek, E. Polatidis, N. Casati, R. Pederson, C. Lyphout, M. Strobl, Influence of laser powder bed fusion scanning pattern on residual stress and microstructure of alloy 718, *Mater. Des.* **221** (2022) 110983.
[19] R. Jiang, A. Mostafaei, Z. Wu, A. Choi, P.W. Guan, M. Chmielus, A.D. Rollett, Effect of heat treatment on microstructural evolution and hardness homogeneity in laser powder bed fusion of alloy 718, *Addit. Manuf*. **35** (2020) 101282.
[20] K. Gruber, R. Dziedzic, B. Kuźnicka, B. Madejski, M. Malicki, Impact of high temperature stress relieving on final properties of Inconel 718 processed by laser powder bed fusion, *Mater. Sci. Eng. A* **813** (2021) 141111.